DOI: 10.1021/ic101150p

Inorganic Chemistry
Article

New Insights into the Factors That Govern the Square/Triangle Equilibria of Pd(II) and Pt(II) Supramolecules. Unexpected Participation of a Mononuclear Species in the Equilibrium

Montserrat Ferrer,[†] Albert Pedrosa,[†] Laura Rodríguez,*[,†] Oriol Rossell,[†] and Marta Vilaseca[‡]

[†]*Departament de Química Inorgànica, Universitat de Barcelona, c/Martí i Franquès 1-11, 08028 Barcelona, Spain, and* [‡]*Mass Spectrometry Core Facility, Institute for Research in Biomedicine, Parc Científic de Barcelona, c/Baldiri Reixac 10-12, 08028 Barcelona, Spain*

Received June 8, 2010

The new rigid fluorinated ligand 4,4′-bis(4-pyridyl)octafluorobiphenyl (**L1**) has been synthesized by a nucleophilic substitution reaction between the organolithium derivative of the 4-bromopyridine and the compound decafluorobiphenyl. The use of **L1** as building block of supramolecular species containing diphosphane or ethylenediamine Pd(II) and Pt(II) fragments has been explored, and the results have been compared with those previously reported for the smaller ligand 1,4-bis(4-pyridyl)tetrafluorobenzene (**L2**). The observed differences (particularly, square/triangle ratio) are discussed in terms of different parameters such as the nature of the ancillary ligands, solvent, or reaction temperature. The synthesis of water-soluble palladium metallamacrocycles derived from **L1** has been attempted using ethylenediamine (en) or tetramethylethylenediamine (tmen) as ancillary ligand. Interestingly, in the latter case, the resulting solutions of the compounds showed, together with the square/triangle equilibrium, the unexpected presence of an additional lower nuclearity species, whose nature has been determined by means of bidimensional ^{1}H NMR experiments.

Introduction

The design and synthesis of discrete molecular architectures via directional self-assembly of polytopic organic donors and metal based acceptors have undergone significant development for more than a decade,[1−7] and it is also a current topic of investigation.[8−23] If *cis*-blocked square-planar metallic centers are used in combination with linear ditopic ligands, squares[24−31] or triangles[32−36] with the metal centers on the corners and the ligands in the edges are the

*To whom correspondence should be addressed. Phone: +34 934031136. Fax: +34 934907725. E-mail: laura.rodriguez@qi.ub.es.

(1) Seidel, S. R.; Stang, P. J. *Acc. Chem. Res.* **2002**, *35*, 972–983.
(2) Leininger, S.; Olenyuk, B.; Stang, P. J. *Chem. Rev.* **2000**, *100*, 853–907.
(3) Jones, C. J. *Chem. Soc. Rev.* **1998**, *27*, 289–299.
(4) Fujita, M. *Chem. Soc. Rev.* **1998**, *27*, 417–425.
(5) Swiegers, G. F.; Malefetse, T. J. *Chem. Rev.* **2000**, *100*, 3483–3537.
(6) Holliday, B. J.; Mirkin, C. A. *Angew. Chem., Int. Ed.* **2001**, *40*, 2022–2043.
(7) Stang, P. J. *Chem.—Eur. J.* **1998**, *4*, 19–27.
(8) Schalley, C. A.; Lutzen, A.; Albrecht, M. *Chem.—Eur. J.* **2004**, *10*, 1072–1080.
(9) Wurthner, F.; You, C. C.; Saha-Moller, C. R. *Chem. Soc. Rev.* **2004**, *33*, 133–146.
(10) Thanasekaran, P.; Liao, R. T.; Liu, Y. H.; Rajendran, T.; Rajagopal, S.; Lu, K. L. *Coord. Chem. Rev.* **2005**, *249*, 1085–1110.
(11) Zangrando, E.; Casanova, M.; Alessio, E. *Chem. Rev.* **2008**, *108*, 4979–5013.
(12) Ferrer, M.; Rodríguez, L.; Rossell, O.; Solans, X. *J. Organomet. Chem.* **2005**, *690*, 1612–1619.
(13) Kraft, S.; Hanuschek, E.; Beckhaus, R.; Haase, D.; Saak, W. *Chem.—Eur. J.* **2005**, *11*, 969–978.
(14) Karadas, F.; Schelter, E. J.; Prosvirin, A. V.; Bacsa, J.; Dunbar, K. R. *Chem. Commun.* **2005**, 1414–1416.
(15) Champin, B.; Sartor, V.; Sauvage, J. P. *New J. Chem.* **2008**, *32*, 1048–1054.
(16) Cotton, F. A.; Liu, C. Y.; Murillo, C. A.; Wang, X. P. *Inorg. Chem.* **2006**, *45*, 2619–2626.
(17) Chen, C.-L.; Zhang, J. Y.; Su, C.-Y. *Eur. J. Inorg. Chem.* **2007**, 2997–3010.
(18) Ghosh, S.; Batten, S. R.; Turner, D. R.; Mukherjee, P. S. *Organometallics* **2007**, *26*, 3252–3255.
(19) Chas, M.; Abella, D.; Blanco, V.; Pía, E.; Blanco, G.; Fernández, A.; Platas-Iglesias, C.; Peinador, C.; Quintela, J. M. *Chem.—Eur. J.* **2007**, *13*, 8572–8582.
(20) Rodriguez, L.; Lodeiro, C.; Lima, J. C.; Crehuet, R. *Inorg. Chem.* **2008**, *47*, 4952–4962.
(21) Rodriguez, L.; Ferrer, M.; Rossell, O.; Coco, S. *J. Organomet. Chem.* **2009**, *694*, 2951–3957.
(22) Sakata, Y.; Hiraoka, S.; Shionoya, M. *Chem.—Eur. J.* **2010**, *16*, 3318–3325.
(23) Ghosh, S.; Mukherjee, P. S. *Inorg. Chem.* **2009**, *48*, 2605–2613.
(24) Rang, A.; Engeser, M.; Maier, N. M.; Nieger, M.; Lindner, W.; Schalley, C. A. *Chem.—Eur. J.* **2008**, *14*, 3855–3859.
(25) Song, L. C.; Jin, G. X.; Wang, H. T.; Zhang, W. X.; Hu, Q. M. *Organometallics* **2005**, *24*, 6464–6471.
(26) Sautter, A.; Kaletas, B. K.; Schmid, D. G.; Dobrawa, R.; Zimine, M.; Jung, G.; van Stokkum, I. H. M.; De Cola, L.; Williams, R. M.; Wurthner, F. *J. Am. Chem. Soc.* **2005**, *127*, 6719–6729.
(27) Rang, A.; Nieger, M.; Engeser, M.; Lutzen, A.; Schalley, C. A. *Chem. Commun.* **2008**, 4789–4791.
(28) Kieltyka, R.; Englebienne, P.; Fakhoury, J.; Autexier, C.; Moitessier, N.; Sleiman, H. F. *J. Am. Chem. Soc.* **2008**, *130*, 10040–10041.

Published on Web 09/24/2010

Chart 1

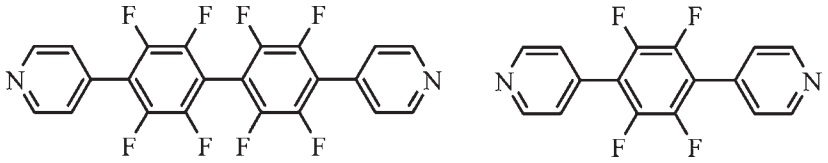

L1 **L2**

favored structures. However, when there is no thermodynamic preference for one species, or when effects like steric strain or electrostatic repulsion are taken into account, two or more species may coexist in dynamic equilibrium in solution. The particular case of the coexistence of molecular squares and triangles in solution has been of great interest in recent years.[37−43] This equilibrium seems to be determined by a sensitive balance between entropy and enthalpy. Because of this balance, the triangle becomes the major component if the ligand's flexibility reduces the strain by allowing the ligand to bend while the square is the major component if the ligands are rigid so that, the enthalpic benefit overcompensates the entropic penalty in square formation. Thus, the reaction of the *cis*-Pt(dppf) corner with 2,7-diazapyrene permitted the synthesis of a square as the unique resulting species,[44] while the use of longer organic edges like 1,4-bis(4-pyridyl)tetrafluorobenzene and 1,4-bis(4-pyridyl)butadiyne gave a mixture of both species in equilibrium.[38,39]

In addition, it has been demonstrated that the equilibria between triangular and square metallacycles also depend on other factors, such as the metal center and its ancillary ligand, the temperature, the concentration, and the solvent.

Unfortunately, in spite of the great number of the reported studies, there are no rules that could help to choose the adequate experimental conditions and the nature of the starting products to control the final composition of the reaction by means of a rational synthesis.

In this work, we would like to go one step further to contribute to clarify a little bit more the factors that lead to these complex square/triangle equilibria. For this goal, we have focused on the analysis of the edge length effect on the formation of either the molecular square or the corresponding triangle.

New molecular polygons were designed and prepared using the rigid fluorinated ligand 4,4′-bis(4-pyridyl)octafluorobiphenyl as an edge (**L1**, Chart 1). This compound presents one more C_6F_4 aromatic ring between the two 4-pyridine units, with respect to the previously reported **L2**,[38] and the structural characteristics of both **L1** and **L2** are similar.

The results of the self-assembly reactions between different diphosphane Pd(II) and Pt(II) triflates and **L1** have been compared with those obtained with **L2** to analyze the effect of the edge length on the composition of the products.

It is important to note that the tetrafluorophenylene units of this edge favor the formation of self-assembled electron-poor cavities that could be used in molecular recognition of electron-rich aromatic compounds.[30,31,42,45−47]

Furthermore, the construction of water-soluble derivatives has been also considered to study the potential applications of the metallacycles in DNA interactions investigations.

Experimental Section

General Procedures. All manipulations were performed under prepurified N_2 using standard Schlenk techniques. All solvents were distilled from appropriate drying agents.

Commercial reagents 1,3-bis(diphenylphosphino)propane (dppp), 1,1′-bis(diphenylphosphino)ferrocene (dppf), decafluorobiphenyl, ethylenediamine, tetramethylethylenediamine were used as received.

The compounds 4-(trimethyltin)pyridine,[48] $[Pt(H_2O)_2(dppp)](OTf)_2$,[49] $[Pd(H_2O)_2(dppp)](OTf)_2$,[49] $[Pt(H_2O)_2(dppf)](OTf)_2$,[44] $[Pd(H_2O)_2(dppf)](OTf)_2$,[44] $[Pd(NO_3)_2(en)]$,[50] $[Pt(NO_3)_2(en)]$,[50] $[Pd(NO_3)_2(tmen)]$[51] and $[Pd(OTf)_2(en)]$[52] were prepared as described previously.

Measurements. Infrared spectra were recorded on a FT-IR 520 Nicolet spectrophotometer. $^{31}P\{^1H\}$ NMR (δ(85% H_3PO_4) = 0.0 ppm), ^{19}F NMR ($\delta(CFCl_3)$ = 0.0 ppm), and one-dimensional (1D)

(29) Blanco, V.; Chas, M.; Abella, D.; Peinador, C.; Quintela, J. M. *J. Am. Chem. Soc.* **2007**, *129*, 13978–13986.
(30) Blanco, V.; Gutiérrez, A.; Platas-Iglesias, C.; Peinador, C.; Quintela, J. M. *J. Org. Chem.* **2009**, *74*, 6577–6583.
(31) Peinador, C.; Pía, E.; Blanco, V.; García, M. D.; Quintela, J. M. *Org. Lett.* **2010**, *12*, 1380–1383.
(32) Zheng, Y. R.; Yang, H. B.; Northrop, B. H.; Ghosh, K.; Stang, P. J. *Inorg. Chem.* **2008**, *47*, 4706–4711.
(33) Willison, S. A.; Krause, J. A.; Connick, W. B. *Inorg. Chem.* **2008**, *47*, 1258–1260.
(34) Tzeng, B. C.; Kuo, J. H.; Lee, Y. C.; Lee, G. H. *Inorg. Chim. Acta* **2008**, *361*, 2515–2521.
(35) Galindo, M. A.; Navarro, J. A. R.; Romero, M. A.; Quiros, M. *Dalton Trans.* **2004**, 1563–1566.
(36) Ghosh, S.; Turner, D. R.; Batten, S. R.; Mukherjee, P. S. *Dalton Trans.* **2007**, 1869–1871.
(37) Sun, Q. F.; Wong, K. M. C.; Liu, L. X.; Huang, H. P.; Yu, S. Y.; Yam, V. W. W.; Li, Y. Z.; Pan, Y. J.; Yu, K. C. *Inorg. Chem.* **2008**, *47*, 2142–2154.
(38) Ferrer, M.; Mounir, M.; Rossell, O.; Ruiz, E.; Maestro, M. A. *Inorg. Chem.* **2003**, *42*, 5890–5899.
(39) Ferrer, M.; Rodríguez, L.; Rossell, O. *J. Organomet. Chem.* **2003**, *681*, 158–166.
(40) Weilandt, T.; Troff, R. W.; Saxell, H.; Rissanen, K.; Schalley, C. A. *Inorg. Chem.* **2008**, *47*, 7588–7598.
(41) Uehara, K.; Kasai, K.; Mizuno, N. *Inorg. Chem.* **2010**, *49*, 2008–2015.
(42) Ferrer, M.; Gutierrez, A.; Mounir, M.; Rossell, O.; Ruiz, E.; Rang, A.; Engeser, M. *Inorg. Chem.* **2007**, *46*, 3395–3406.
(43) Hollo-Sitkei, E.; Tarkanyi, G.; Parkanyi, L.; Megyes, T.; Besenyei, G. *Eur. J. Inorg. Chem.* **2008**, 1573–1583.
(44) Stang, P. J.; Olenyuk, B.; Fan, J.; Arif, A. M. *Organometallics* **1996**, *15*, 904–908.
(45) Kasai, K.; Aoyagi, M.; Fujita, M. *J. Am. Chem. Soc.* **2000**, *122*, 2140–2141.
(46) Fujita, M.; Yazaki, J.; Ogura, K. *Tetrahedron Lett.* **1991**, *32*, 5589–5592.
(47) Fujita, M.; Ogura, K. *Coord. Chem. Rev.* **1996**, *148*, 249–264.
(48) Phillips, J. E.; Herber, R. H. *J. Organomet. Chem.* **1984**, *268*, 39–47.
(49) Stang, P. J.; Chen, K.; Arif, A. M. *J. Am. Chem. Soc.* **1995**, *117*, 6273–6283.
(50) Orita, A.; Jiang, L. S.; Nakano, T.; Ma, N. C.; Otera, J. *Chem. Commun.* **2002**, 1362–1363.
(51) Stang, P. J.; Cao, D. H.; Saito, S.; Arif, A. M. *J. Am. Chem. Soc.* **1995**, *117*, 6273–6283.
(52) Adrian, R. A.; Zhu, S.; Powell, D. R.; Broker, G. A.; Tiekink, E. R. T.; Walmsley, J. A. *Dalton Trans.* **2007**, 4399–4404(we used H_2O/EtOH, 1:1 as solvent instead of H_2O).

and two-dimensional (2D) ^{1}H NMR (δ(TMS) = 0.0 ppm) spectra were obtained on a spectrometers at 25 °C unless otherwise stated. A ledbpgs2s (2D sequence with bipolar gradients for diffusion using stimulated echo and LED) was used for the diffusion experiment.[53] Electrospray mass spectra were recorded on a LC/MSD-TOF (Agilent Technologies) spectrometer at the Universitat de Barcelona and on a LTQ-FT Ultra (Thermo Scientific) at the Biomedical Research Institute (PCB-Universitat de Barcelona). Elemental analyses of C, H, N, and S were carried out at the Serveis Científico-Tècnics in Barcelona.

Molecular Modeling and Semiempirical Calculations. Geometry optimization of the molecules was calculated with PM3 semiempirical methods included in the software package Spartan'04 V1.0.0.

Synthesis and Characterization. Synthesis of 4,4′-Bis(4-pyridyl)-octafluorobiphenyl (L1). *n*-BuLi (10.1 mL, 16.2 mmol) was added dropwise to a precooled (−78 °C) diethylether solution (20 mL) of 4-bromopyridine (15.0 mmol) prepared from 3 g (15.0 mmol) of 4-bromopyridine hydrochloride.[54] After 30 min of stirring the solution was allowed to warm to −40 °C, and the initial beige solution turned pale pink after 2 h. A solution of decafluorobiphenyl (1.71 g, 5.10 mmol) in diethylether (30 mL) was then added, and a Bourdeaux color was immediately acquired. The resulting mixture was allowed to warm to room temperature. After 24 h of stirring, the solution was treated with an aqueous solution of NH_4Cl and extracted with CH_2Cl_2 until the aqueous phase became colorless. The organic phase was concentrated to dryness, washed with diethylether and cold dichloromethane, and 1.0 g of a pale beige solid was obtained (43% yield).

^{1}H NMR (400.1 MHz, $CDCl_3$, 298 K), δ(ppm): 8.83 (d, J(H−H) = 6.0 Hz, 4H, $H_{\alpha-pyr}$), 7.48 (d, J(H−H) = 6.0 Hz, 4H, $H_{\beta\text{-pyr}}$). ^{19}F-RMN (376.5 MHz, $CDCl_3$, 298 K), δ(ppm): −137.6 (m, 4F, F_A), −142.3 (m, 4F, F_B). ES-MS(+): m/z = 453.1 ([M+H]$^+$, calcd: 453.1). IR (KBr, cm^{-1}): 1585 (C═N), 1456 (C═C), 971 (C−F). Anal. Found.: C, 58.45; H, 1.80; N; 6.23. Calcd: C, 58.41; H, 1.77; N, 6.19.

Synthesis of Square [Pd(dppp)(L1)]$_4$(OTf)$_8$/Triangle [Pd(dppp)-(L1)]$_3$(OTf)$_6$ (1a/1b). A solution of $[Pd(H_2O)_2(dppp)](OTf)_2$ (17 mg, 0.02 mmol) in CH_3NO_2 (4 mL) was added to a suspension of 4,4′-bis(4-pyridyl)octafluorobiphenyl (9 mg, 0.02 mmol) in CH_3NO_2 (2 mL). The resulting mixture was stirred at room temperature for 1 h and then, 4 mL of diethylether were added to precipitate 24 mg of **1a**/**1b** as a pale yellow solid (93% yield).

1a: ^{1}H NMR (400.1 MHz, acetone-d_6, 298 K), δ(ppm): 9.27 (d, J(H−H) = 6.0 Hz, 16 H, $H_{\alpha\text{-pyr}}$), 7.85−7.43 (m, 96 H, Ph + $H_{\beta\text{-pyr}}$), 3.44 (brs, 16 H, -P-***CH*$_2$-CH$_2$), 2.43 (brs, 8 H, -P-CH$_2$-***CH*$_2$**). ^{31}P NMR (101.3 MHz, acetone-d_6, 298 K), δ(ppm): 7.4 (s). ^{19}F NMR (376.5 MHz, acetone-d_6, 298 K), δ(ppm): −144.0 (m, 16 F, F_A), −147.5 (m, 16 F, F_B).

1b: ^{1}H NMR (400.1 MHz, acetone-d_6, 298 K), δ(ppm): 9.15 (brs, 12 H, $H_{\alpha\text{-pyr}}$), 7.85−7.43 (m, 72 H, Ph + $H_{\beta\text{-pyr}}$), 3.44 (brs, 12 H, -P-***CH*$_2$-CH$_2$), 2.43 (brs, 6 H, -P-CH$_2$-***CH*$_2$**). ^{31}P NMR (101.3 MHz, acetone-d_6, 298 K), δ(ppm): 8.1 (s). ^{19}F NMR (376.5 MHz, acetone-d_6, 298 K), δ(ppm): −144.2 (m, 12 F, F_A), −147.8 (m, 12 F, F_B).

1a/1b: ES-MS(+) m/z = 2389.1 ([**1a** − 2(OTf)]$^{2+}$, calcd: 2389.1), 1754.1 ([**1b** − 2(OTf)]$^{2+}$, calcd: 1754.6), 1119.1 ([Pd(dppp)(**L1**)-(OTf)]$^+$, calcd: 1119.1). Anal. Calcd for $(C_{51}H_{34}F_{14}N_2O_6P_2PdS_2)n$ (1268.4·n): C, 48.25; H, 2.68; N, 2.20; S, 5.05. Found: C, 48.32; H, 2.66; N, 2.17; S, 5.07.

Synthesis of Square [Pt(dppp)(L1)]$_4$(OTf)$_8$/Triangle [Pt(dppp)-(L1)]$_3$(OTf)$_6$ (2a/2b). A solution of $[Pt(H_2O)_2(dppp)](OTf)_2$ (19 mg, 0.02 mmol) in CH_3NO_2 (4 mL) was added dropwise to a suspension of 4,4′-bis(4-pyridyl)octafluorobiphenyl (9 mg, 0.02 mmol) in CH_3NO_2 (2 mL). The resulting mixture was warmed to 60 °C and stirred for 5 h, and then, 3 mL of diethylether were added to precipitate 24 mg of **2a**/**2b** as an orange solid (90% yield).

2a: ^{1}H NMR (400.1 MHz, acetone-d_6, 298 K), δ(ppm): 9.33 (d, J(H−H) = 5.6 Hz, 16 H, $H_{\alpha\text{-pyr}}$), 7.89−7.45 (m, 80 H, Ph), 7.55 (d, J(H−H) = 5.6 Hz, 16 H, $H_{\beta\text{-pyr}}$), 3.54 (brs, 16 H, -P-***CH*$_2$-CH$_2$−), 2.41 (brs, 8 H, -P-CH$_2$-***CH*$_2$**). ^{31}P NMR (101.3 MHz, acetone-d_6, 298 K), δ(ppm): −14.8 (s, J(P−Pt) = 3035 Hz). ^{19}F NMR (376.5 MHz, acetone-d_6, 298 K), δ(ppm): −139.7 (m, 16 F, F_A), −143.1 (m, 16 F, F_B).

2b: ^{1}H NMR (400.1 MHz, acetone-d_6, 298 K), δ(ppm): 9.22 (d, J(H−H) = 5.6 Hz, 12 H, $H_{\alpha\text{-pyr}}$), 7.89−7.45 (m, 96 H, Ph + $H_{\beta\text{-pyr}}$), 3.54 (brs, 12 H, -P-***CH*$_2$-CH$_2$), 2.41 (brs, 6 H, -P-CH$_2$-***CH*$_2$**). ^{31}P NMR (101.3 MHz, acetone-d_6, 298 K), δ(ppm): −14.3 (s, J(P−Pt) = 3035 Hz). ^{19}F NMR (376.5 MHz, acetone-d_6, 298 K), δ(ppm): −139.9 (m, 12 F, F_A), −143.4 (m, 12 F, F_B).

2a/2b: ES-MS(+) m/z = 1887.7 ([**2b** − 2OTf]$^{2+}$, calcd: 1887.7), 1661.5 ([**2a** − 3OTf]$^{3+}$, calcd: 1661.2), 1208.1 ([**2a** − 4OTf]$^{4+}$, [**2b** − 3OTf]$^{3+}$, ([Pt(dppp)(**L1**)(OTf)]$^+$, calcd: 1208.1). Anal. Calcd for $(C_{51}H_{34}F_{14}N_2O_6P_2PtS_2)n$ (1357.09·n): C, 45.10; H, 2.51; N, 2.06; S, 4.72. Found: C, 45.15; H, 2.49; N, 2.08; S, 4.74.

Synthesis of Square [Pd(dppf)(L1)]$_4$(OTf)$_8$ /Triangle [Pd(dppf)-(L1)]$_3$(OTf)$_6$ (3a/3b). A solution of $[Pd(H_2O)_2(dppf)](OTf)_2$ (20 mg, 0.02 mmol) in dichloromethane (4 mL) was added dropwise to a suspension of 4,4′-bis(4-pyridyl)octafluorobiphenyl (9 mg, 0.02 mmol) in dichloromethane (2 mL). After 2 h of stirring at room temperature, the solution was concentrated to about 3 mL and diethylether (4 mL) was added to precipitate 25 mg of **3a/3b** as a violet solid (90% yield).

3a: ^{1}H NMR (250.1 MHz, $CDCl_3$, 298 K), δ(ppm): 9.12 (brs, 16 H, $H_{\alpha\text{-pyr}}$), 7.94−7.59 (m, 80 H, Ph), 7.16 (brs, 16 H, $H_{\beta\text{-pyr}}$), 4.91 (brs, 16 H, $H_{\alpha\text{-Cp}}$), 4.64 (brs, 16 H, $H_{\beta\text{-Cp}}$). ^{31}P NMR (101.3 MHz, $CDCl_3$, 298 K), δ(ppm): 33.6 (s). ^{19}F NMR (282.2 MHz, $CDCl_3$, 298 K), δ(ppm): −136.1 (m, 16 F, F_A), −141.3 (m, 16 F, F_B).

3b: ^{1}H NMR (250.1 MHz, $CDCl_3$, 298 K), δ(ppm): 9.02 (brs, 12 H, $H_{\alpha\text{-pyr}}$), 7.94−7.59 (m, 60 H, Ph), 7.12 (d, J(H−H) = 5.0 Hz, 12 H, $H_{\beta\text{-pyr}}$), 4.91 (brs, 12 H, $H_{\alpha\text{-Cp}}$), 4.64 (brs, 12 H, $H_{\beta\text{-Cp}}$). ^{31}P NMR (101.3 MHz, $CDCl_3$, 298 K), δ(ppm): 34.1 (s). ^{19}F NMR (282.2 MHz, $CDCl_3$, 298 K), δ(ppm): −136.3 (m, 12 F, F_A), −141.5 (m, 12 F, F_B).

3a/3b: ES-MS(+) m/z = 1966.0 ([**3b** − 2OTf]$^{2+}$, calcd: 1967.0), 1731.7 ([**3a** − 3OTf]$^{3+}$, calcd: 1732.0), 1263.1 ([Pd(dppf)(**L1**)-(OTf)]$^+$, calcd: 1262.0). Anal. Calcd for $(C_{58}H_{36}F_{14}FeN_2O_6P_2PdS_2)n$ (1410.25·n): C, 49.35; H, 2.55; N, 1.99; S, 4.54. Found: C, 49.39; H, 2.57; N, 2.01; S, 4.56.

Synthesis of Square [Pt(dppf)(L1)]$_4$(OTf)$_8$/Triangle [Pt(dppf)-(L1)]$_3$(OTf)$_6$ (4a/4b). $[Pt(H_2O)_2(dppf)](OTf)_2$ (22 mg, 0.02 mmol) and 4,4′-bis(4-pyridyl)octafluorobiphenyl (9 mg, 0.02 mmol) were reacted and worked up as described for **3a**/**3b** to yield 28 mg (95% yield) of an orange product.

4a: ^{1}H NMR (400.1 MHz, $CDCl_3$, 298 K), δ(ppm): 9.19 (d, J(H−H) = 5.0 Hz, 16 H, $H_{\alpha\text{-pyr}}$), 7.90−7.56 (m, 80 H, Ph), 7.20 (d, J(H−H) = 5.0 Hz, 16 H, $H_{\beta\text{-pyr}}$), 4.87 (brs, 16 H, $H_{\alpha\text{-Cp}}$), 4.61 (brs, 16 H, $H_{\beta\text{-Cp}}$). ^{31}P NMR (101.3 MHz, $CDCl_3$, 298 K), δ(ppm): 3.9 (s, J(P−Pt) = 3417 Hz). ^{19}F NMR (376.5 MHz, $CDCl_3$, 298 K), δ(ppm): −136.1 (m, 16 F, F_A), −141.3 (m, 16 F, F_B).

4b: ^{1}H NMR (400.1 MHz, $CDCl_3$, 298 K), δ(ppm): 9.08 (d, J(H−H) = 5.0 Hz, 12 H, $H_{\alpha\text{-pyr}}$), 7.90−7.56 (m, 60 H, Ph), 7.17 (d, J(H−H) = 5.0 Hz, 12 H, $H_{\beta\text{-pyr}}$), 4.87 (brs, 12 H, $H_{\alpha\text{-Cp}}$), 4.61 (brs, 12 H, $H_{\beta\text{-Cp}}$). ^{31}P NMR (101.3 MHz, $CDCl_3$, 298 K), δ(ppm): 4.2 (s, J(P−Pt) = 3417 Hz). ^{19}F NMR (376.5 MHz, $CDCl_3$, 298 K), δ(ppm): −136.3 (m, 12 F, F_A), −141.6 (m, 12 F, F_B).

4a/4b: ES-MS(+) m/z = 1851.1 ([**4a** − 3OTf]$^{3+}$, calcd: 1850.4), 1351.1 ([Pt(dppf)(**L1**)(OTf)]$^+$, [**4a** − 4OTf]$^{4+}$, [**4b** − 3OTf]$^{3+}$; calcd: 1350.7). Anal. Calcd for $(C_{58}H_{36}F_{14}FeN_2O_6P_2PtS_2)n$ (1498.94·n): C, 46.43; H, 2.40; N, 1.87; S, 4.27. Found: C, 46.47; H, 2.42; N, 1.88; S, 4.29.

(53) Wu, D. H.; Chen, A. D.; Johnson, C. S. *J. Magn. Reson., Ser. A* **1995**, *115*, 260–264.

(54) 4-Bromopyridine hydrochloride was treated with NaOH in H_2O. Et_2O was added, and the resulting 4-bromopyridine ethereal solution was dried over $MgSO_4$ and CaH_2 and taken to dryness under vacuum.

Scheme 1. Synthesis of **L1** Following a Nucleophilic Aromatic Substitution Reaction

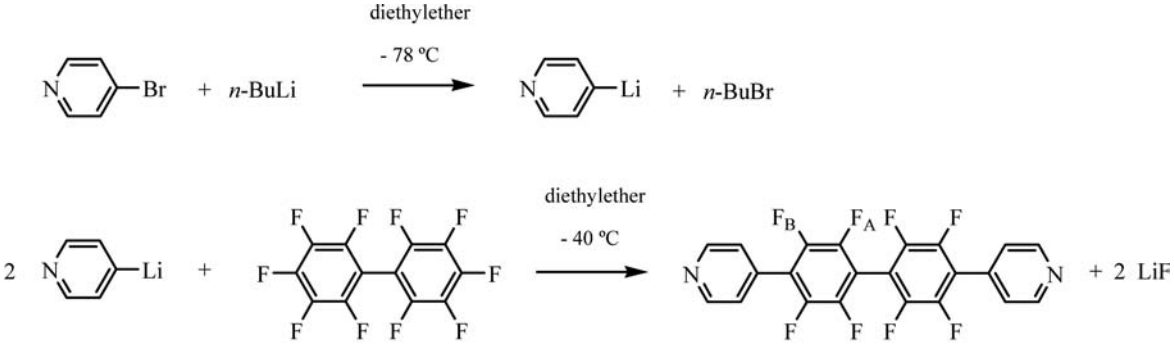

L1

Synthesis of Square [Pd(en)(L1)]$_4$(NO$_3$)$_8$ (5a). 4,4′-Bis(4-pyridyl)octafluorobiphenyl (9 mg, 0.02 mmol) was added to a suspension of [Pd(NO$_3$)$_2$(en)] (6 mg, 0.02 mmol) in dichloromethane (10 mL). After 2 days of stirring at 35 °C, the solid residue was filtered, and the compound was obtained as a beige solid. Small quantities of starting materials were also present, and it was no possible to obtain **5a** as a pure solid.

^{1}H NMR (250.1 MHz, D$_2$O, 298 K), δ(ppm): 8.89 (brs, 16 H, H$_{\alpha\text{-pyr}}$), 7.92 (brs, 16 H, H$_{\beta\text{-pyr}}$), 2.82 (s, 16 H, (CH$_2$)$_{en}$). ^{19}F NMR (376.5 MHz, D$_2$O, 298 K), δ(ppm): −138.2 (m, 16 F, F$_A$), −143.0 (m, 16 F, F$_B$).

Synthesis of Square [Pd(en)(L1)]$_4$(OTf)$_8$/Triangle [Pd(en)(L1)]$_3$(OTf)$_6$ (6a/6b). To a suspension of 4,4′-bis(4-pyridyl)-octafluorobiphenyl (9 mg, 0.02 mmol) in acetonitrile (2 mL) was added a solution of [Pd(OTf)$_2$(en)] (9 mg, 0.02 mmol) in 8 mL of the same solvent. After 2 h of stirring, the yellow suspension gave a beige solution which was concentrated to dryness to obtain 17 mg of **6a**/**6b** (90% yield).

6a: ^{1}H NMR (250.1 MHz, CD$_3$CN, 298 K), δ(ppm): 9.00 (d, J(H−H) = 5.0 Hz, 16 H, H$_{\alpha\text{-pyr}}$), 7.80 (d, J(H−H) = 5.0 Hz, 16 H, H$_{\beta\text{-pyr}}$), 4.39 (brs, 16 H, (NH$_2$)$_{en}$), 2.89 (s, 16 H, (CH$_2$)$_{en}$). ^{19}F NMR (376.5 MHz, CD$_3$CN, 298 K), δ(ppm): −144.1 (m, 16 F, F$_A$), −148.1 (m, 16 F, F$_B$).

6b: ^{1}H NMR (250.1 MHz, CD$_3$CN, 298 K), δ(ppm): 8.80 (d, J(H−H) = 5.0 Hz, 12 H, H$_{\alpha\text{-pyr}}$), 7.60 (brs, 12 H, H$_{\beta\text{-pyr}}$), 4.39 (brs, 16 H, (NH$_2$)$_{en}$), 2.80 (s, 12 H, (CH$_2$)$_{en}$). ^{19}F NMR (376.5 MHz, CD$_3$CN, 298 K), δ(ppm): −144.8 (m, 12 F, F$_A$), −148.5 (m, 12 F, F$_B$).

6a/6b: Anal. Calcd for (C$_{26}$H$_{16}$F$_{14}$N$_4$O$_6$PdS$_2$)n (916.4·n): C, 34.04; H, 6.25; N, 6.11; S, 6.98. Found: C, 34.07; H, 6.27; N, 6.13; S, 6.99.

Synthesis of Square [Pd(tmen)(L1)]$_4$(NO$_3$)$_8$/Triangle [Pd(tmen)(L1)]$_3$(NO$_3$)$_6$/[Pd(tmen)(L1)] (7a/7b/7c). Solid 4,4′-bis(4-pyridyl)-octafluorobiphenyl (9 mg, 0.02 mmol) was added to a solution of [Pd(NO$_3$)$_2$(tmen)] (7 mg, 0.02 mmol) in deuterated methanol (2 mL). After 1 day of stirring the suspension was filtered, and then, the solution was concentrated to dryness to obtain 14 mg of **7a/7b/7c** in 85% yield.

7a: ^{1}H NMR (500.1 MHz, CD$_3$OD, 298 K), δ(ppm): 9.45 (d, J(H−H) = 10 Hz, 16 H, H$_{\alpha\text{-pyr}}$), 7.99 (d, J(H−H) = 10 Hz, 16H, H$_{\beta\text{-pyr}}$), 3.15 (s, 16 H, (CH$_2$)$_{tmen}$), 2.74 (s, 48 H, (CH$_3$)$_{tmen}$). ^{19}F NMR (376.5 MHz, CD$_3$OD, 298 K), δ(ppm): −139.6 (m, 16 F, F$_A$), −143.8 (m, 16 F, F$_B$).

7b: ^{1}H NMR (500.1 MHz, CD$_3$OD, 298 K), δ(ppm): 9.37 (d, J(H−H) = 10 Hz, 12 H, H$_{\alpha\text{-pyr}}$), 7.92 (d, J(H−H) = 10 Hz, 12 H, H$_{\beta\text{-pyr}}$), 3.18 (s, 12 H, (CH$_2$)$_{tmen}$), 2.85 (s, 36 H, (CH$_3$)$_{tmen}$). ^{19}F NMR (376.5 MHz, CD$_3$OD, 298 K), δ(ppm): −139.8 (m, 12 F, F$_A$), −144.0 (m, 12 F, F$_B$).

7c: ^{1}H NMR (500.1 MHz, CD$_3$OD, 298 K), δ(ppm): 9.22 (t, 2 H, H$_\alpha$-coord-pyr), 8.77 (t, 2 H, H$_\beta$-coord-pyr), 8.01 (sh, 2 H, H$_\alpha$-uncoord-pyr), 7.69 (dd, 2 H, H$_\beta$-uncoord-pyr), 3.04 (s, br, 2 H, (CH$_2$)$_{tmen}$), 2.98 (s, br, 2 H, (CH$_2$)$_{tmen}$), 2.78 (s, 3 H, (CH$_3$)$_{tmen}$), 2.77 (s, 3 H, (CH$_3$)$_{tmen}$), 2.68 (s, 3 H, (CH$_3$)$_{tmen}$), 2.67 (s, 3 H, (CH$_3$)$_{tmen}$). ^{19}F NMR (376.5 MHz, CD$_3$OD, 298 K), δ(ppm): −139.8 (m, 2 F, F$_A$-coord-pyr), −140.4 (m, 2 F, F$_B$-coord-pyr), −143.8 (m, 2 F, F$_A$ uncoord-pyr), −144.5 (m, 2 F, F$_B$-uncoord-pyr).

7a/7b/7c: Anal. Calcd for (C$_{28}$H$_{24}$F$_8$N$_6$O$_6$Pd)n (798.4·n): C, 42.08; H, 3.00; N, 10.52. Found: C, 42.11; H, 3.02; N, 10.54.

Results and Discussion

Synthesis of the Linear Organic Edge 4,4′-Bis(4-pyridyl)octafluorobiphenyl (L1). The synthesis of the new 4,4′-bis(4-pyridyl)octafluorobiphenyl ligand (**L1**) was attempted following the two experimental procedures reported for the synthesis of **L2**: (i) a palladium-catalyzed cross-coupling reaction[38] between the Grignard reagent 1,4-dibromooctafluorobiphenyldimagnesium and 2 equiv of 4-bromopyridine and (ii) a reaction of [PdCl$_2$(PPh$_3$)$_2$]/LiCl-promoted cross-coupling between 2 equiv of 4-pyridyltrimethylstannane and 1,4-dibromooctafluorobiphenyl.[55,56] Unfortunately, these methods did not allow the formation of **L1** in good yields since monopyridyl derivatives were found as the major products of the reaction.

However, we found that a double nucleophilic aromatic substitution reaction of the lithium derivative of the 4-bromopyridine with decafluorobiphenyl, in diethylether at −40 °C, permitted the successful synthesis of **L1** in moderate yield (45%) (Scheme 1). It is interesting to take into account that low temperature favors the formation of the desired disubstituted product while higher temperatures seem to form a mixture of mono- and di- and trisubstituted products.[57] The 3:1 stoichiometry is also important to avoid the formation of byproducts.

The use of different spectroscopic techniques and mass spectrometry support the formation of **L1**. Thus, the ^{1}H NMR spectrum displays two peaks at 8.83 and 7.48 ppm that correspond to the H$_\alpha$ and H$_\beta$ protons of the pyridine units while ^{19}F NMR spectrum shows the absence of the *para*-fluorine atoms because of their substitution by the pyridine groups. Moreover, ES-MS(+) spectrometry shows a peak at m/z 453.1 due to the formation of the [**L1** + H$^+$] species.

(55) Ferrer., M.; Gutiérrez, A.; Mounir, M.; Solans, X.; Font-Bardía, M. *Acta Crystallogr.* **2006**, *E62*, 03213–o3214.

(56) Fujita, M.; Oka, H.; Ogura, K. *Tetrahedron Lett.* **1995**, *36*, 5247–5250.

(57) Geramita, K.; McBee, J.; Tao, Y.; Segalman, R. A.; Tilley, T. D. *Chem. Commun.* **2008**, 5107–5109.

Scheme 2. Self-Assembly Reactions between **L1** and the Diphosphane Metal Corners

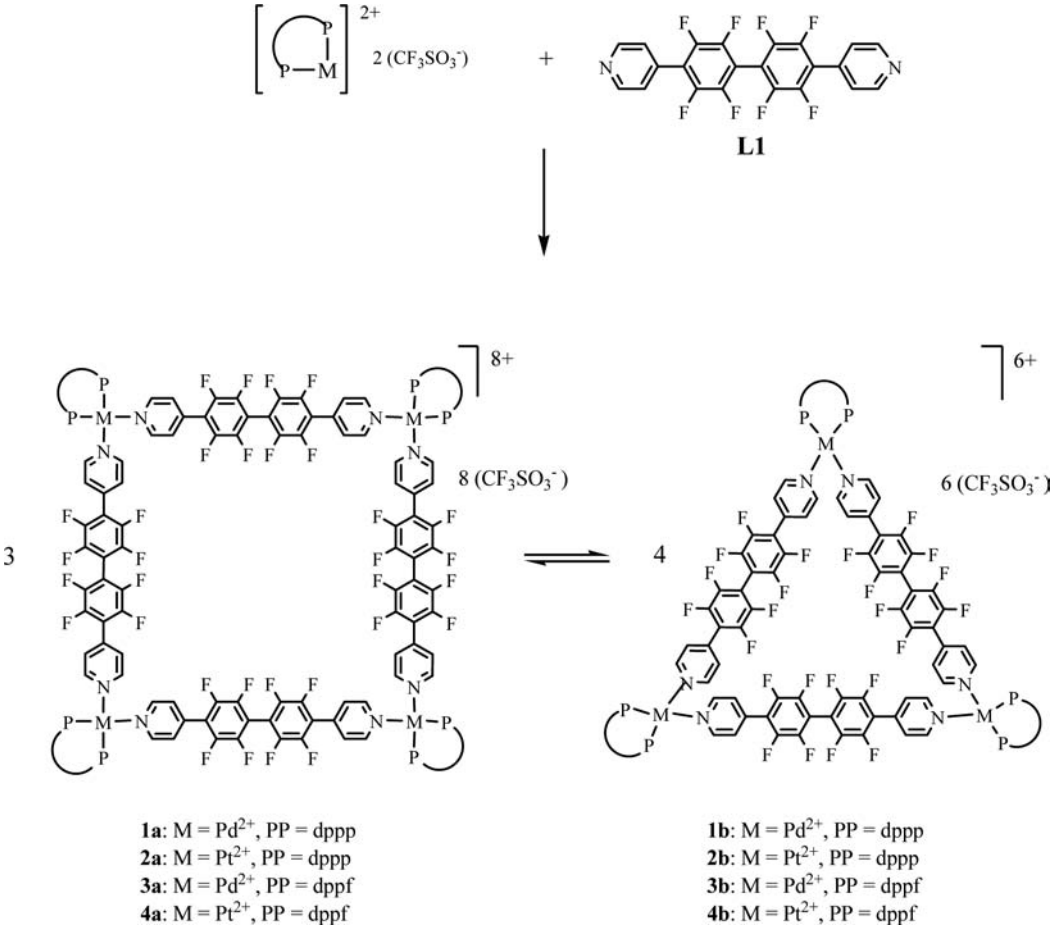

Synthesis and Characterization of Diphosphane Metallacycles. $[M(dppp)(H_2O)_2](OTf)_2$ and $[M(dppf)(H_2O)_2](OTf)_2$ (M = Pd, Pt) were reacted with equimolar amounts of **L1** in acetone and nitromethane (for the dppp derivatives) or in dichloromethane (for the dppf derivatives) at room temperature. ^{31}P, ^{19}F, and ^{1}H NMR spectra showed the assembly of two main products with highly symmetric structures (Scheme 2).

To clarify our results, we will discuss separately the experiments with both diphosphanes.

The reactions carried out with the dppp derivatives led to the formation of both macrocyclic square and triangle in equilibrium almost in all cases. In particular, the reaction of the palladium complex $[Pd(dppp)(H_2O)_2](OTf)_2$ with **L1** in acetone showed the formation of two symmetrical products (**1a**/**1b**), whose $^{31}P\{^{1}H\}$ NMR spectrum showed signals at 7.4 ppm, assigned to the square (**1a**), and at 8.1 ppm, corresponding to the triangle (**1b**) (Supporting Information, Figure S1). The observed about 11 ppm upfield shift with respect to the palladium starting product is due to the coordination of the pyridine rings to the metal atoms.[58] The assignment of the species in the equilibrium is based on the concentration effects on the square/triangle ratio according to Le Chatelier's law, being the square the main species at all concentrations.

(58) Jude, H.; Disteldorf, H.; Fischer, S.; Wedge, T.; Hawkridge, A. M.; Arif, A. M.; Hawthorne, M. F.; Muddiman, D. C.; Stang, P. J. *J. Am. Chem. Soc.* **2005**, *127*, 12131–12139.

^{1}H and ^{19}F NMR spectra also show the presence of both species in equilibrium (see Supporting Information, Figures S2 and S3).

The **1a**/**1b** system provides an interesting example of the decisive role of the solvent in shifting the square/triangle equilibrium. Indeed, the $^{31}P\{^{1}H\}$ NMR spectrum of the same reaction in nitromethane displays a unique peak at 5.11 ppm, assigned to the square metallacycle, in contrast with the mixture of triangular and square species observed in acetone. This behavior agrees with the idea that the use of a less polar solvent favors the formation of the triangle.[40]

The reactions with the platinum derivative to obtain the compounds **2a**/**2b** required higher temperature (60 °C) and longer reaction times (5 h) with respect to those of palladium, because of the lower lability of the platinum metal center. In this case, an equilibrium between **2a** and **2b** is observed in both acetone and nitromethane, although the square/triangle ratio is shifted to the triangular macrocycle in acetone.

Our results using palladium and platinum dppf derivatives are as follows. The reaction between $[M(dppf)(H_2O)_2](OTf)_2$ (M = Pd, Pt) with **L1** in dichloromethane led to a square/triangle equilibrium in both cases (**3a/3b** and **4a/4b**). $^{31}P\{^{1}H\}$ NMR spectrum of **3a/3b**, recorded at the same concentration used for **1a/1b**, clearly shows that the concentration of both metallacycles is not very different (Figure 1), the triangular species being more favored than in the case of dppp. This behavior is due to the different bite angle of the diphosphanes.

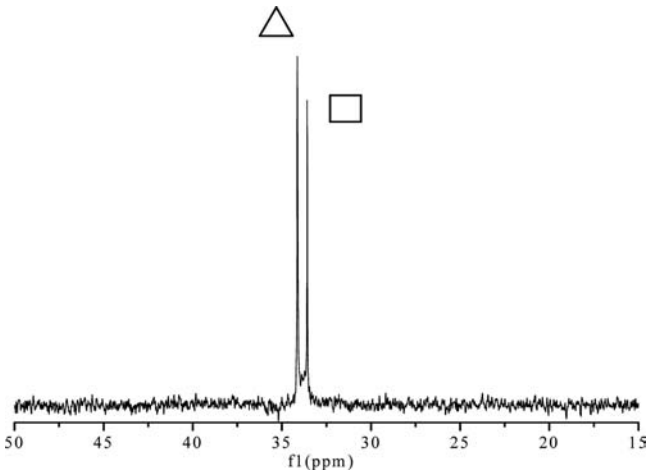

Figure 1. $^{31}P\{^{1}H\}$ NMR spectrum of **3a**/**3b** in $CDCl_3$.

^{1}H and ^{19}F NMR spectra support our results. For example, Figure 2 shows the corresponding ^{1}H NMR spectrum where the H_α and H_β of the pyridine groups are clearly assigned.

The square/triangle molar ratios obtained for all these reactions at different concentrations in nitromethane were also analyzed, and the results are summarized in Table 1. An inspection of this Table leads us to observe that, as expected, the reactions with the diphosphane dppp (compounds **1** and **2**), with smaller bite angle (91.56°),[59] yield the preferred formation of the supramolecular square, while the use of the diphosphane dppf (compounds **3** and **4**), with larger bite angle (98.74°),[59] favors the formation of the triangle. These results were also observed with **L2**.

At this point, it is interesting to note that a comparison with the results reported for the square/triangle **L2** derivatives[38] shows, in contrast with our expectations, that the use of the longer and more flexible edge **L1** shifts the square/triangle equilibria to the square species. In fact, the square is the only self-assembled metallacycle (**1a**) obtained from the reaction of palladium dppp-containing corner and **L1** in nitromethane (see Table 1).

As a conclusion, these studies show that the use of a longer and more flexible edge does not seem to have a clear effect on the preferred formation of the triangle versus the corresponding square.

Since NMR showed the presence of two symmetrical species in the solution, high resolution ESI-MS spectrometry has been used to confirm the ring size of the macrocycles. Although the spectra were recorded in nitromethane and in acetone, the latter allowed the observation of suitable peaks for all the macrocycles while nitromethane only led to good results for **2a**/**2b**. This fact was also observed and carefully analyzed by Engeser et al.[60] who suggested that acetone is probably a good compromise between a polar solvent, which helps to dissociate the ion pairs during the electrospray process, and unpolar solvents, which allow the ions to desolvate easily because of low surface tension and high vapor pressures.

The ESI-MS spectrum of **1a**/**1b** and **2a**/**2b** recorded in acetone displays multiply charged cations verifing the formation of the expected macrocycles Figure S4 (Supporting Information) and Figure 3, respectively. In Figure 3, the signal at m/z 1661.49 corresponds to the molecular peak of the square with the loss of three triflate anions while the peak at m/z 1887.67 is due to the presence of the triangle with the loss of two triflate anions. There is also observed a peak at m/z 1208.13 that displays an isotope pattern resulting from the superposition of the quadruply charged square, the triply charged triangle, and the mononuclear fragment $[Pt(dppp)(\mathbf{L1})(OTf)]^{+}$.

The superposition of different charged species is frequently observed for these kind of metallacycles, and in our case it was also shown for the Pt dppf derivative (Supporting Information, Figure S5).

DOSY Measurements. DOSY NMR experiments with ^{1}H detection were also performed to ascertain the simultaneous existence of both the square and the triangle supramolecules in solution. Systems **3a**/**3b** and **4a**/**4b** were chosen for this study because of the relatively large separation between the resonances of the α-protons (and in lesser extend, the β-protons) of the pyridine units for each pair of species.

Although we expected that larger structures should have smaller diffusion coefficients than smaller ones, DOSY NMR experiments showed two sets of signals with almost the same diffusion coefficient (Supporting Information, Figure S6).

This result could be traced back to the different time scale in the ^{1}H and DOSY NMR experiments. Although the exchange process between both species in equilibrium is quite slow in ^{1}H NMR experiments, this phenomenon become faster in the DOSY NMR which works with a diffusion delay in its sequence.[23,40]

As expected, the exchange process became slower at low temperature (223 K), and two different diffusion coefficients could be clearly observed for **4a**/**4b** (Figure 4).

The results are in agreement with the assignment of the corresponding peaks of the square and the triangle since the smaller diffusion coefficients correspond to the larger species.

DOSY experiments let us evaluate the relative size of both molecules considering them as encapsulating spheres[61] for which the hydrodynamic radius can be calculated by means of purely geometrical considerations.[40,62−64] The calculated quotient between the experimental diffusion coefficients of **4a** and **4b** is 0.84. Taking into account that the triangle/square r_H ratio has to be equal to 0.82, our result is in good agreement with the theoretical value and thus, with the assignment of the square and triangle entities.

In contrast, DOSY NMR experiments with the analogous palladium compounds **3a**/**3b** did not give similar results since ^{1}H NMR at 223 K spectrum showed that

(59) Dierkes, P.; van Leeuwen, P. W. N. M. *J. Chem. Soc., Dalton Trans.* **1999**, 1519–1529.
(60) Engeser, M.; Rang, A.; Ferrer, M.; Gutierrez, A.; Baytekin, H. T.; Schalley, C. A. *Int. J. Mass Spectrom.* **2006**, *255*, 185–194.
(61) Otto, W. H.; Keefe, M. H.; Splan, K. E.; Hupp, J. T.; Larive, C. K. *Inorg. Chem.* **2002**, *41*, 6172–6174.
(62) Pastor, A.; Martinez-Viviente, E. *Coord. Chem. Rev.* **2008**, *252*, 2314–2345.
(63) Floquet, S.; Brun, S.; Lemonnier, J. F.; Henry, M.; Delsuc, M. A.; Prigent, Y.; Cadot, E.; Taulelle, F. *J. Am. Chem. Soc.* **2009**, *131*, 17254–17259.
(64) Macchioni, A.; Ciancaleoni, G.; Zuccaccia, C.; Zuccaccia, D. *Chem. Soc. Rev.* **2008**, *37*, 479–489.

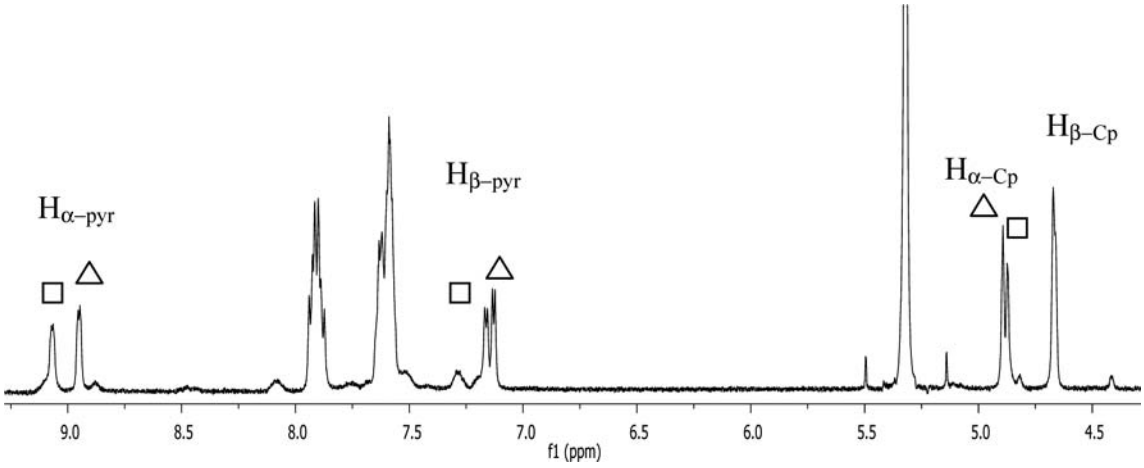

Figure 2. ^{1}H NMR spectrum of **3a**/**3b** in $CDCl_3$.

Table 1. Square/Triangle Ratios Obtained for the Different Diphosphane Derivatives in Nitromethane at Different Concentrations

compound	3 mM	10 mM	20 mM
1a/1b	1−0	1−0	1−0
2a/2b	3−1	5−1	5−1
3a/3b	1−2	1−1.6	1.3−1
4a/4b	1−2	1−1.6	1.3−1

the equilibrium was completely displaced to the enthalpically favored species (square). Variable temperature ^{1}H NMR suggested that the diffusion experiment could be performed at 268 K (Supporting Information, Figure S7), but no separation between the signals were observed (Supporting Information, Figure S8). These results are indicative of the fast triangle-square exchange in the more labile palladium compounds.

Molecular Modeling. To produce single crystals for X-ray crystal structure determination is a very difficult task when there are species in equilibrium. To complete the characterization of the complexes, semiempirical PM3 calculations were carried out with the Spartan program. Since the compounds only differ in the diphosphane linked to the metal atom, the minimum conformation geometries were calculated for the dppf metallacycles, and the main calculated parameters are expected to be similar for the dppp derivatives.

The calculated geometry of compounds **4a** and **4b** are depicted in Figure 5.

Figure 5 shows that the four (square) or the three (triangle) metal atoms are located in the same plane, the pyridine rings are perpendicular to this plane, and the twisting between the two tetrafluorobenzene moieties is approximately 50°. $\pi-\pi$ interactions between the pyridine and the phenyl rings of the diphosphane are expected to occur since the reported distance for these interactions between two parallel planes is 3.3−3.8 Å[65] and, in our case, the calculated distances are about 3.4 Å for the square and 3.6 Å for the triangle.

It could be observed that the compounds present a big empty inner cavity, whose size (19.7 Å × 19.7 Å for the square and 20.3 Å × 18.0 Å for the triangle) has been estimated by measuring the distance between the opposite platinum atoms of both edges. These M···M distances evidence that the size of these metallacycles is similar to that calculated for $[(CO)_3ClRe(pyC{\equiv}CC_6H_2(OC_{12}H_{25})_2C{\equiv}Cpy)]_4$ (20.60−20.90 Å)[66] and quite larger than that reported for other square or triangular metallacycles, such as $[(tmen)Pd(pyC=Cpy)]_3(NO_3)_6$ (13.30−13.38 Å),[41] $[(tmen)Pd(pyC{\equiv}Cpy)]_3(NO_3)_6$ (13.52−13.65 Å),[41] $[(PMe_3)_2Pt(pyC=Cpy)]_3(X)_6$ (X = OTf^-, $CoB_{18}C_4H_{22}^-$; 13.32−13.55 Å),[67] $[(dppp)Pt(pyC=Cpy)]_3(OTf)_6$,[40] $[(phen)(PEt_3)_4Pt_2(bipy)]_3(OTf)_6$ (17.10−18.04 Å),[68] $[(CO)_3ClRe(pyC=Cpy)]_4$ (13.90−14.40 Å),[66] and $[Pd(en)(4,4'\text{-bipy})]_n(NO_3)_{2n}$ (n = 3, 4; 15.50 Å).[43]

The calculated N−M−N angles are between 85° and 86° for the square and between 65° and 66° for the triangles, which are in the range of those reported in the literature for analogous supramolecular systems.[40,69,70]

Synthesis and Characterization of Ethylenediamine Metallacycles. The nature of the ancillary ligand on the metal corners seems to play an important role in the self-assembled products of the reaction. For this reason, we decided to extend our studies by changing the diphosphanes by ethylenediamine groups. The use of ethylenediamine N-donor ligands, not only provides electronic changes but also allows for the production of water-soluble macrocycles. These effects were previously observed by us with the **L2** derivatives, where the use of the ethylenediamine ancillary ligand rendered the formation of the square for both palladium and platinum derivatives.[42] These single self-assembled compounds were used as hosts for the recognition of aromatic electron-rich guests in water,[42] and, moreover, the platinum derivative was assayed as intercalator in DNA structure as a possible anticancer drug.[71] These results encouraged us to synthesize new larger water-soluble complexes and study

(65) Kammer, S.; Muller, H.; Grunwald, N.; Bellin, A.; Kelling, A.; Schilde, U.; Mickler, W.; Dosche, C.; Holdt, H. *Eur. J. Inorg. Chem.* **2006**, 1547–1551.

(66) O'Donnell, J. L.; Zuo, X.; Goshe, A. J.; Sarkisov, L.; Snurr, R. Q.; Hupp, J. T.; Tiede, D. M. *J. Am. Chem. Soc.* **2007**, *129*, 1578–1585.

(67) Schweiger, M.; Seidel, R.; Arif, A. M.; Stang, P. J. *Inorg. Chem.* **2002**, *41*, 2556–2559.

(68) Megyes, T.; Jude, H.; Grósz, T.; Bakó, I.; Radnai, T.; Tárkányi, G.; Pálinkás, G.; Stang, P. J. *J. Am. Chem. Soc.* **2005**, *127*, 10731–10738.

(69) Stang, P. J.; Persky, N. E. *Chem. Commun.* **1997**, 77–78.

(70) Sautter, A.; Schmid, D. G.; Jung, G.; Wurthner, F. *J. Am. Chem. Soc.* **2001**, *123*, 5424–5430.

(71) Mounir, M.; Lorenzo, J.; Ferrer, M.; Prieto, M. J.; Rossell, O.; Aviles, F. X.; Moreno, V. *J. Inorg. Biochem.* **2007**, *101*, 660–666.

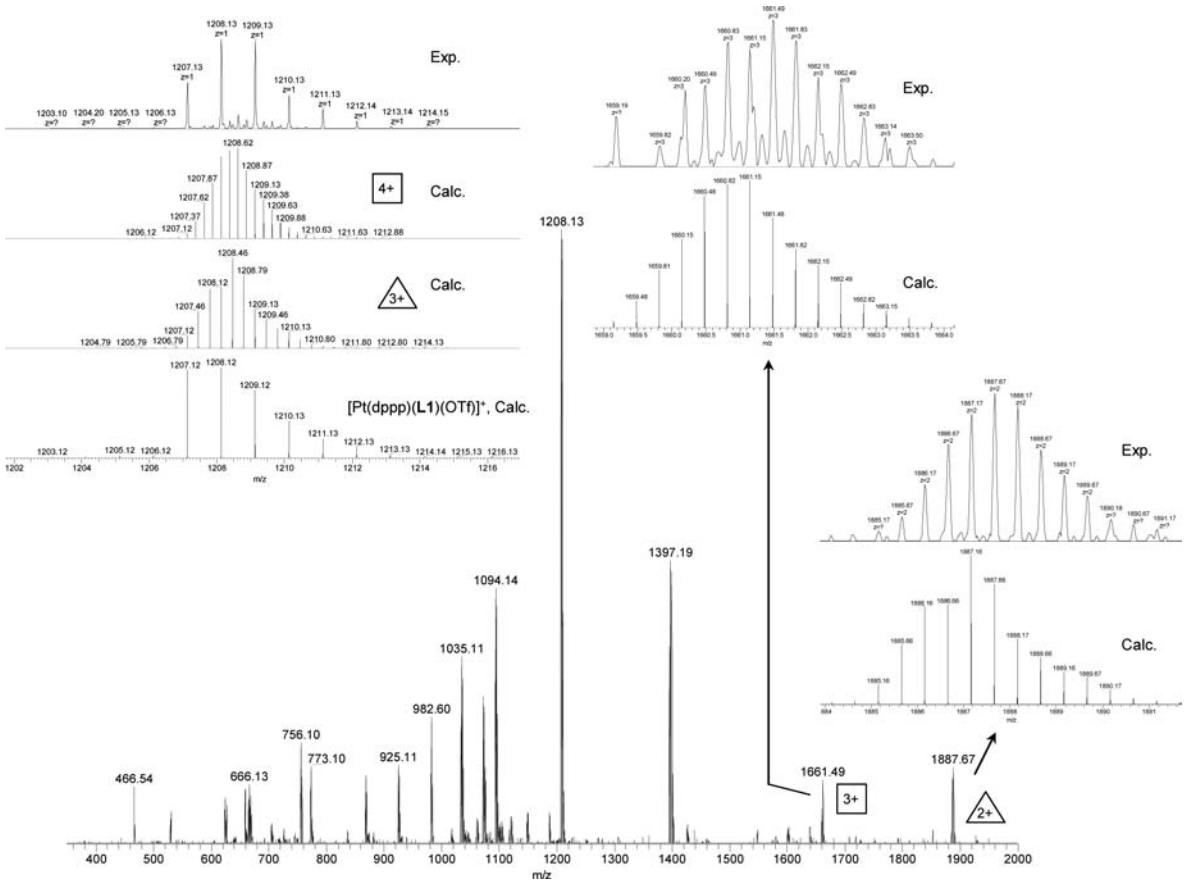

Figure 3. ESI-MS spectrum of **2a**/**2b** in acetone.

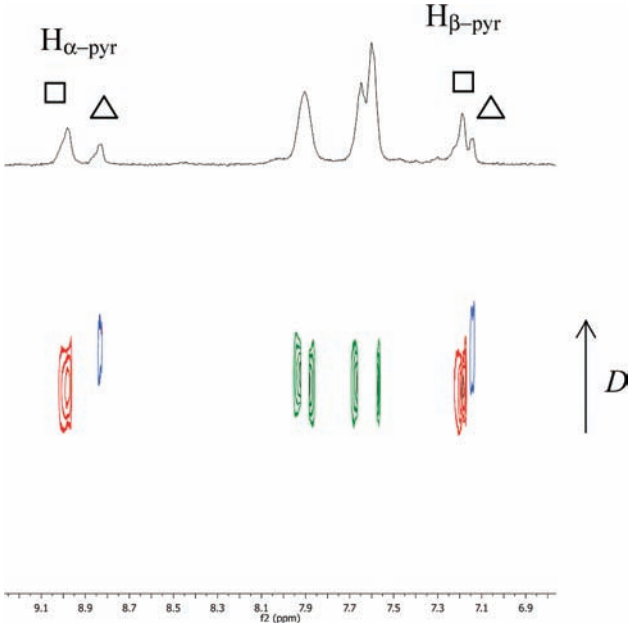

Figure 4. ^{1}H-DOSY NMR spectrum of **4a**/**4b** in CD_2Cl_2 at 223 K.

their potential effect on host−guest properties and DNA interactions, to compare the effect of the size of the metallacycles on these applications.

All attempts to obtain the ethylenediamine platinum derivative were unsuccessful, while the corresponding palladium compound was obtained with both nitrate and triflate counterions (Supporting Information, Scheme S1).

Figure 5. Minimum energy geometry calculated for compound **4a** (left) and **4b** (right) (hydrogens are omitted for clarity).

Different methods were assayed for the synthesis of the ethylenediamine palladium metallacycles, and the best result was obtained from the reaction of **L1** with a dichloromethane suspension of $[Pd(NO_3)_2(en)]$ at 35 °C for 2 days. ^{1}H NMR characterization showed the formation of a unique new symmetrical species (**5a**) together with the presence of few amounts of the starting products. As occurred for other nitrate macrocycles,[42] no ESI-MS signals were observed for this compound, and we propose the obtained macrocycle to be a molecular square on the basis of literature reports.[72−74] These results indicate that

(72) Fujita, M.; Tominaga, M.; Hori, A.; Therrien, B. *Acc. Chem. Res.* **2005**, *38*, 369–378.
(73) Wurthner, F.; You, C. C.; Saha-Moller, C. R. *Chem. Soc. Rev.* **2004**, *33*, 133–146.
(74) Lindoy, L. F.; Atkinson., I. M. *Coord. Chem. Rev.* **2000**, *200*, 207–215.

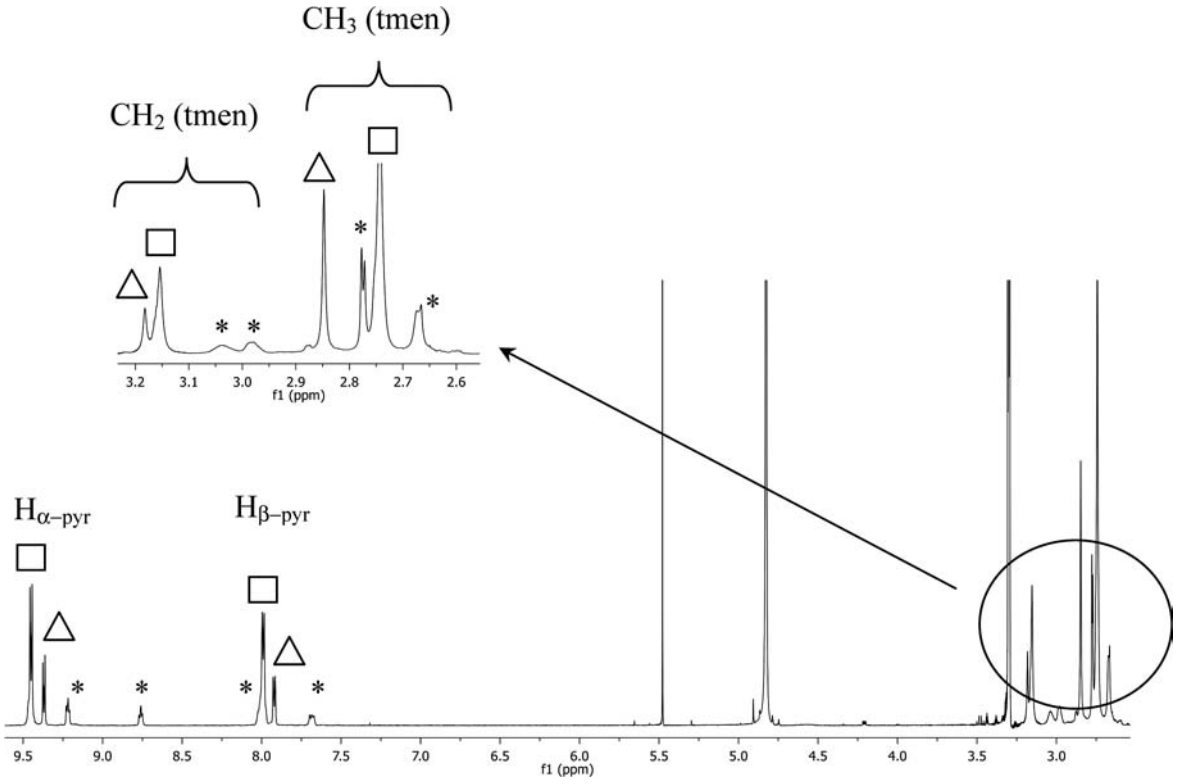

Figure 6. ^{1}H NMR spectrum of 7**a**/**7b**/**7c** in CD_3OD.

the reaction was not complete, possibly because of the low solubility of the $[Pd(NO_3)_2(en)]$ in organic solvents. For this reason, we decided to proceed with the synthesis of the analogous triflate macrocycle by means of the same procedure but using $[Pd(OTf)_2(en)]$ instead of $[Pd(NO_3)_2$-(en)]. The subsequent addition of $(NBu_4)NO_3$ should yield the formation of **5a**. The synthesis of the triflate self-assembled species with **L1** showed the formation of two products in equilibrium (**6a**/**6b**, Supporting Information, Figure S9), but unfortunately, the exchange process between the triflate and the nitrate anions was not successful, preventing the formation of the water-soluble macrocycle **5a**.

To go one step further on the synthesis of water-soluble supramolecules, we planned to improve the solubility of the palladium and platinum metal corners in organic solvents to facilitate the completion of the reaction in dichloromethane. Thus, the ancillary ligand "en" was changed by the closely related "tmen" while keeping the nitrate counterion to ensure water solubility. As for "en" derivatives, platinum tmen self-assembled species could not be obtained, but the palladium complexes were carefully analyzed.

The reaction of $[Pd(NO_3)_2(tmen)]$ with **L1** was performed in methanol and surprisingly, ^{1}H NMR characterization showed not only the formation of the square and the triangle **7a**/**7b** in equilibrium (Figure 6) but also the presence of another unidentified product (**7c**, marked with an asterisk in this figure).

The use of longer reaction time and/or changes in the polarity of the solvent (dichloromethane instead of methanol) led to similar results. ^{1}H NMR spectrum recorded at different concentrations lead us to conclude that the unexpected product is involved in the same equilibrium. That is, ^{1}H NMR spectrum showed a reversible behavior where the intensity of these new peaks increases in the same magnitude at diluted solutions which seems to indicate that all of them correspond to a unique product of low nuclearity (Supporting Information, Figure S10).

It is interesting to remark that, although square/triangle equilibria are well studied in the literature,[37−43] the simultaneous formation of low nuclearity products is scarcely detected.[19,43] In particular, similar observations have been recently reported by Besenyei and co-workers for the reaction of $[Pd(NO_3)_2(tmen)]$ with the 4,4′-bipyridine edge at low concentrations.[43] This species was proposed to be a less symmetrical component but its nature was not elucidated.

To explore this reaction, and in particular, the effect of the ancillary ligand on the final composition of the products, we decided to react $[Pd(NO_3)_2(tmen)]$ with the 4,4′-bis(4-pyridyl)tetrafluorobenzene edge (**L2**). ^{1}H and ^{19}F NMR spectra at different concentrations displayed once more the formation of an equilibrium between both square and triangular macrocycles together with the asymmetrical species. Since this behavior does not seem to be observed with less sterically hindered ethylenediamine derivatives, all these results seem to indicate that the bulky tmen is the responsible one for the formation of a third species that is also present in the equilibrium.

It is interesting to notice that the predesigned reaction between 1 equiv of metal corner with 1 equiv of a linear edge gives, in general, the spontaneous assembly of closed supramolecular complexes instead of open low nuclearity compounds. This new species could behave as a precursor for the synthesis of more complex structures, so its formation and identification is of great interest. As a consequence, different experiments have been performed to determine the nature of this new species.

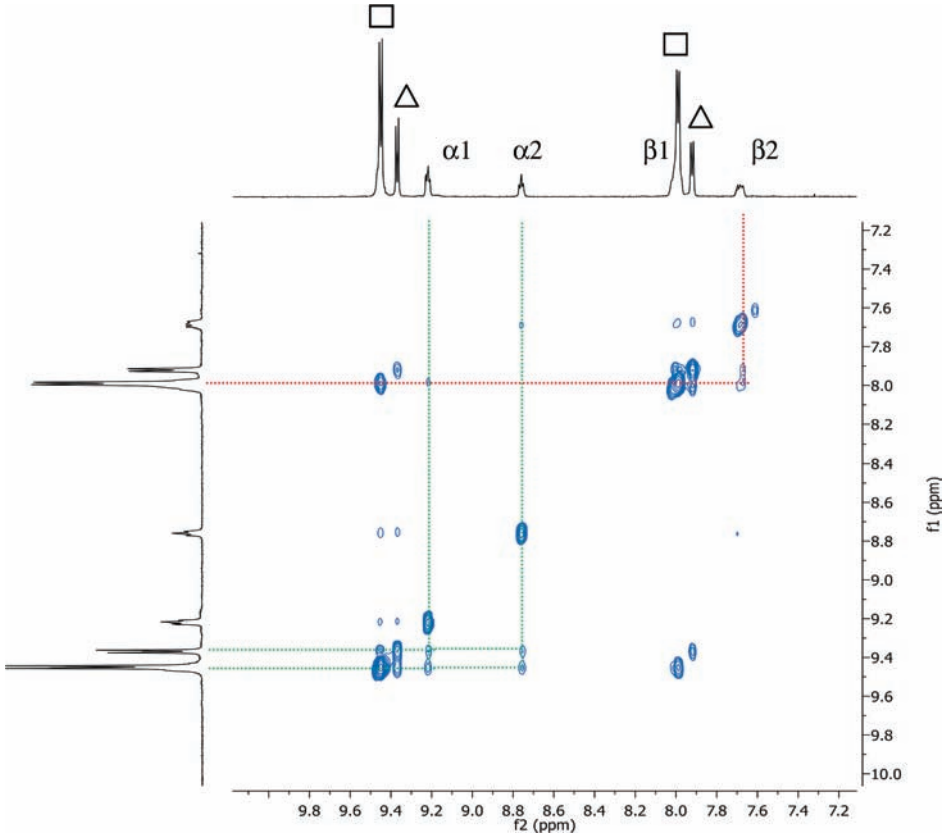

Figure 7. $^1H-^1H$ NOESY spectrum of **7a**/**7b**/**7c** in CD_3OD.

First, $^1H-^1H$ NOESY spectrum confirms the existence of a dynamic equilibrium between the macrocycles and the lower nuclearity species. It is clearly demonstrated by the presence of exchange peaks between the H_α protons of the new species ($\alpha1$ and $\alpha2$) and the H_α pyridyl protons of the macrocycles (green color, Figure 7) and of those corresponding to the exchange of $\beta1$ and $\beta2$ with the H_β of the macrocycles (red color, Figure 7).

Obviously, these signals could not be attributed to spatially close correlation peaks, giving us an evidence of the existence of a dynamic equilibrium between the lower nuclearity species and the macrocycles, but it does not provide us any information about the nature of the mononuclear product.

Second, ^1H DOSY NMR characterization of the sample carried out at room temperature shows the presence of two different sets of signals (Supporting Information, Figure S11) that correspond to the smaller species and to both macrocycles respectively. Low temperature diffusion experiments could not be carried out since at low temperatures the NMR peaks of the smaller species disappear (Supporting Information, Figure S12). Although diffusion experiments evidenced that the unidentified species is smaller than the macrocycles, the exchange rate between the triangle and the square was too fast at room temperature to have an accurate characterization in terms of DOSY NMR experiments.

Third, ^1H and ^{19}F NMR display the presence of four unequivalent pyridine protons and fluorine atoms respectively, which is indicative of the formation of a non-symmetrical species. Two possible mononuclear fragments would agree with these NMR data, that is, the $[Pd(\mathbf{L1})(X)(tmen)]^{n+}$ moiety (for X = solvent, n = 2; for X = counterion, n = 1) (Figure 8, A), or an angular palladium fragment $[Pd(\mathbf{L1})_2(tmen)]^{2+}$ (Figure 8, B).

Both products have to present H_α and H_β pyridyl protons at similar displacement to those of the pyridine protons of **L1** (labeled $\alpha2$ and $\beta2$ in the figure) and also, two pyridyl protons downfield shifted, because of the coordination to the metal atom (labeled $\alpha1$ and $\beta1$ in the figure). ^1H NMR spectrum of both species only should differ at the upfield region (tmen) since two unequivalent methylene and methyl protons have to be observed only for **A**. A carefully inspection of Figure 6 supports the formation of this particular product due, to the presence of two signals, at 2.98 and 3.04 ppm, corresponding to the methylene groups. The definitive proof for the identification of the mononuclear species was obtained by $^1H-^1H$-COSY NMR that shows a coupling between the CH_2 groups of the tmen (Supporting Information, Figure S13), which is only in agreement with the presence of $[Pd(\mathbf{L1})(X)(tmen)]^{n+}$ (Scheme 3).

In conclusion, the use of the tmen palladium corner has lead to the formation of a complex equilibrium between three species that have been identified as square and triangular metallacycles and a new unexpected mononuclear compound, which has been assigned to the asymmetrical mononuclear cation $[Pd(\mathbf{L1})(X)(tmen)]^{n+}$ (X = solvent or counteranion) by means of 1D and 2D ^1H NMR and ^{19}F NMR experiments. The presence and identification of this new species is remarkable since, to our knowledge, it has not been characterized previously and shows the unexpected formation of a single bond between one metal corner unit and one edge unit instead of the formation of the closed metallacyclic structures.

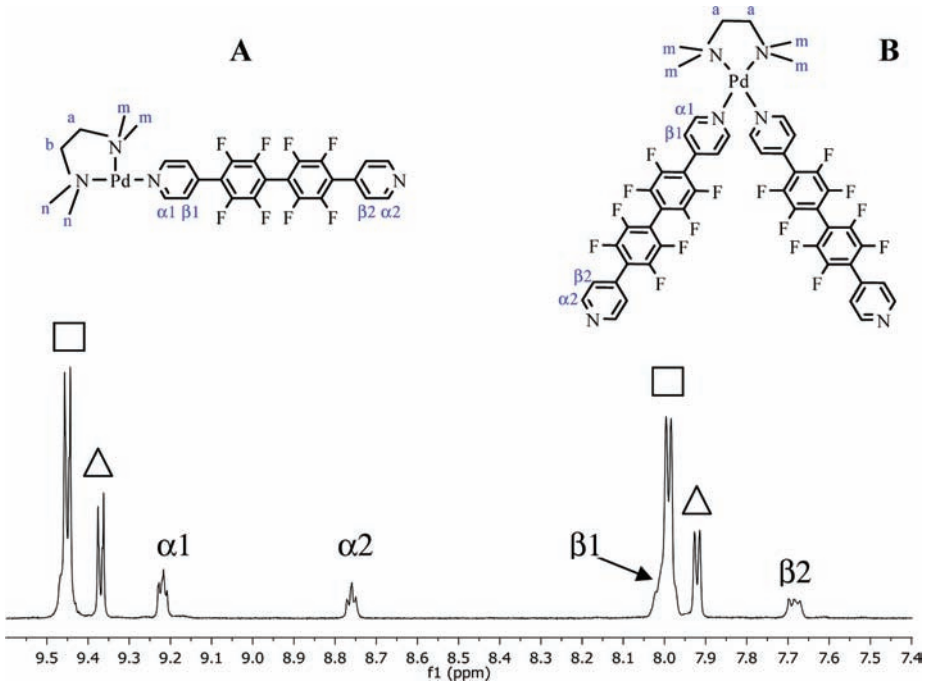

Figure 8. ^{1}H NMR region of the H_α and H_β pyridyl protons of the species present in the equilibrium together with a representation of the two possible lower nuclearity obtained compounds.

Scheme 3. Self-Assembly Reaction between **L1** and $[Pd(NO_3)_2(tmen)]$

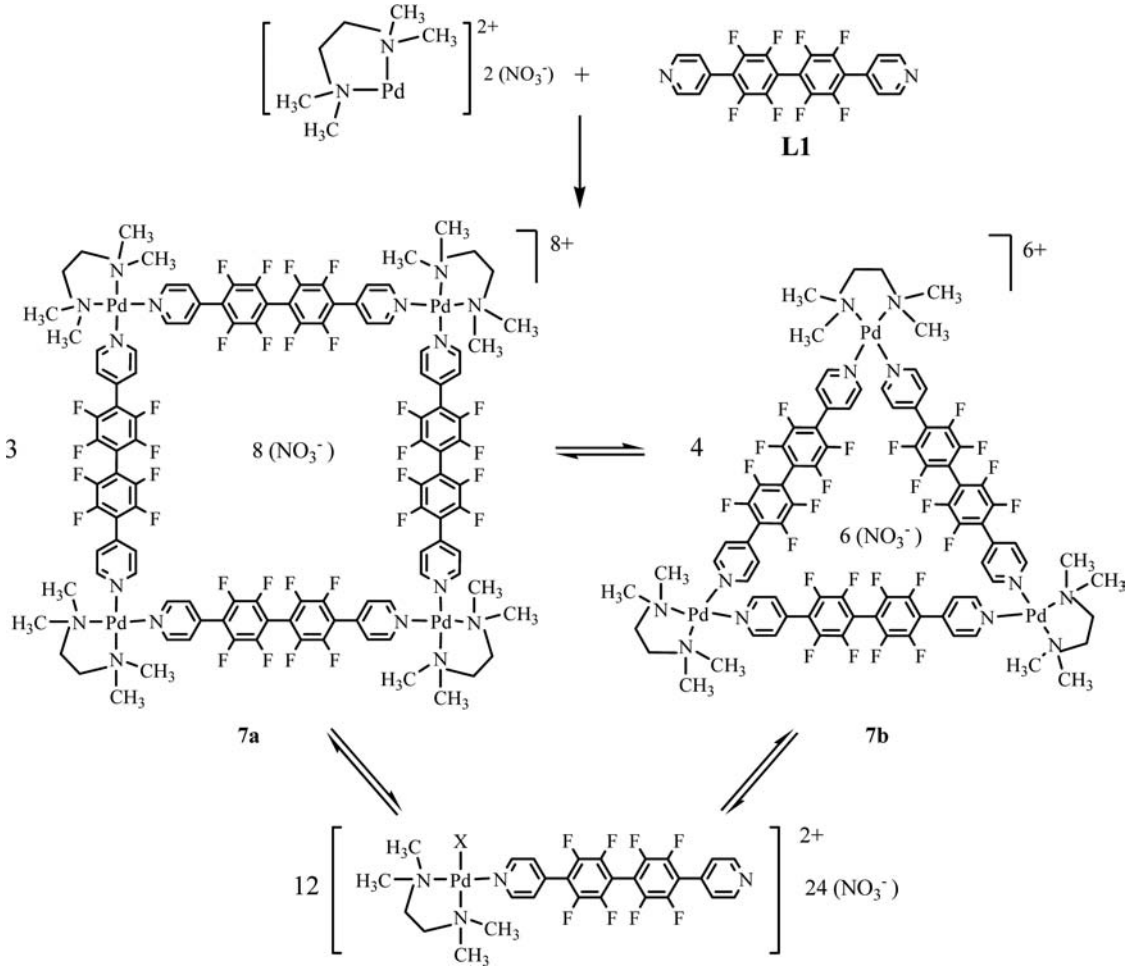

Conclusions

The new 4,4′-bis(4-pyridyl)octafluorobiphenyl ditopic ligand **L1** has been synthesized following a nucleophilic aromatic substitution reaction between the organolithium derivative of the 4-bromopyridine and the decafluorobiphenyl compound. The use of this ligand as an edge in self-assembly reactions with palladium and platinum $[M(PP)(H_2O)_2](OTf)_2$ (PP = dppp, dppf) corners leads to the formation of an equilibrium between square and triangular macrocycles in all cases, the main product being the square. The square/triangle ratios obtained in this work compare well with those reported in previous studies using the shorter 1,4-bis(4-pyridyl)tetrafluorobenzene (**L2**) edge. Unexpectedly, the use of **L1**, as a more flexible and longer edge, did not increase the relative concentration of the triangular species versus the corresponding square.

^{1}H-DOSY NMR experiments at low temperature on the dppf palladium and platinum supramolecules only exhibited a good separation between square and triangular macrocycles in the case of the platinum derivatives. The higher lability of the palladium derivatives facilitates a faster triangle-square exchange.

The self-assembly reactions between **L1** and the ethylenediamine type corners $[Pd(X)_2(NN)]$ ($X^- = NO_3^-$, OTf^-; NN = en, tmen) provided diverse results. While the reaction between $[Pd(NO_3)_2(en)]$ and **L1** rendered the formation of the square macrocycle exclusively, the use of the corresponding triflate derivative $[Pd(NO_3)_2(en)]$ yielded an equilibrium between the square and triangle.

Unexpectly, the reaction between $[Pd(NO_3)_2(tmen)]$ and **L1** yielded three different species in equilibrium, that is, the square, the triangle, and a lower nuclearity species. ^{1}H−^{1}H-COSY NMR has been very helpful to determine the nature of the mononuclear species as the asymmetrical $[Pd(\mathbf{L1})(X)(tmen)]^{n+}$ fragment. The formation of this mononuclear species has not been previously reported in the literature, and it is of great interest since it could behave as a precursor for the synthesis of more complex supramolecular structures.

Acknowledgment. Financial support for this research was provided by the Ministerio de Ciencia e Innovación of Spain (Project CTQ2009-08795).

Supporting Information Available: $^{31}P\{^1H\}$ NMR spectrum of **1a**/**1b** in acetone-d_6 (Figure S1), ^{1}H NMR spectrum of **1a**/**1b** in acetone-d_6 (Figure S2), ^{19}F NMR spectrum of **1a**/**1b** in acetone-d_6 (Figure S3), ESI-MS spectrum of **1a/1b** in acetone (Figure S4), ESI-MS spectrum of **4a/4b** in acetone (Figure S5), ^{1}H-DOSY NMR spectrum of **4a**/**4b** in CD_2Cl_2 at 298 K (Figure S6), ^{1}H NMR spectra of **3a**/**3b** in CD_2Cl_2 at different temperatures (Figure S7), ^{1}H-DOSY NMR spectrum of **3a**/**3b** in CD_2Cl_2 at 268 K (Figure S8), ^{1}H NMR spectrum of **6a**/**6b** in CD_3CN (Figure S9), ^{1}H NMR spectrum of **7a**/**7b**/**7c** in CD_3OD at diluted conditions (Figure S10), ^{1}H−^{1}H DOSY spectrum of **7a**/**7b**/**7c** in CD_3OD (Figure S11), ^{1}H NMR spectrum of 7**a**/**7b**/**7c** in CD_3OD at different temperatures (Figure S12), ^{1}H−^{1}H COSY spectrum of **7a**/**7b**/**7c** in CD_3OD (expanded region), (Figure S13), ^{1}H−^{1}H COSY spectrum of **7a**/**7b**/**7c** in CD_3OD (full spectrum), (Figure S14), self-assembly reactions between **L1** and the ethylenediamine metal corners (Scheme S1). This material is available free of charge via the Internet at http://pubs.acs.org.